

Highly Water-Dispersible Biocompatible Magnetite Particles with Low Cytotoxicity Stabilized by Citrate Groups**

Jia Liu, Zhenkun Sun, Yonghui Deng,* Ying Zou, Chunyuan Li, Xiaohui Guo, Liqin Xiong, Yuan Gao, Fuyou Li, and Dongyuan Zhao*

The synthesis of functional nanoparticles with controllable size and shape is of great importance because of their fundamental scientific significance and broad technological applications.^[1–6] Magnetic nanocrystals have attracted much attention in the past few decades owing to their unique magnetic features and important applications in biomedicine^[7–12] and therapeutics.^[13–18] In particular, superparamagnetic nanoparticles have been extensively pursued for bio-separation,^[19] drug delivery,^[9,20] and detection of cancer.^[10,21–22] Among various magnetic nanoparticles, iron oxides, such as magnetite (Fe₃O₄) or maghemite (γ -Fe₂O₃), have been considered as ideal candidates for these bio-related applications owing to their good biocompatibility and stability in physiological conditions and low cytotoxicity.^[23]

Many methods have been developed to prepare iron oxide nanocrystals.^[24] The thermal decomposition of organometallic and coordination compounds in nonpolar solution has been used successfully for the synthesis of monodisperse magnetic nanocrystals with high crystallinity and small size on the nanometer scale.^[25] However, the magnetic nanocrystals synthesized by these methods are usually hydrophobic, stabilized by nondegradable surfactants, and have a low magnetization, which hampers their applications extremely in bio-related fields, where water-dispersible particles with high magnetic field responsiveness are in demand. Therefore, much effort has focused on the fabrication of water-soluble iron oxide nanocrystals with controllable sizes, fast magnetic response, and desirable surface properties. Although many ligand-exchange strategies have been explored to offer them hydrophilic surface and aqueous dispersibility, their magnetic field responsiveness has not been effectively improved.^[26–29]

Li and co-workers reported a convenient synthesis of hydrophilic magnetite microspheres by a solvothermal reaction by reduction of FeCl₃ with ethylene glycol (EG), but the resultant magnetite microspheres are ferromagnetic and not water dispersible.^[30] Recently, they synthesized magnetic microspheres using a microemulsion of oil droplets in water as confined templates. These magnetic nanoparticles are assembled with the evaporation of low-boiling-point solvents.^[31] More recently, by using high-temperature reduction reaction with poly(acrylic acid) (PAA) as a stabilizer, FeCl₃ as a precursor, and diethylene glycol as a reductant, Ge et al.^[32] directly fabricated water-dispersible superparamagnetic nanocrystal clusters with controllable diameters of 30–180 nm. These nanoclusters are composed of small nanocrystals of 6–8 nm. However, the polyelectrolyte PAA attached on the magnetic clusters is not biodegradable and biocompatible, and thus may limit their applications. Herein, we report a facile synthesis of highly water-dispersible magnetite particles with tunable size by a modified solvothermal reaction.

The magnetite particles were synthesized by a modified solvothermal reaction at 200 °C by reduction of FeCl₃ with EG in the presence of sodium acetate as an alkali source and biocompatible trisodium citrate (Na₃Cit) as an electrostatic stabilizer. The excess EG acts as both the solvent and reductant.^[30] Na₃Cit was chosen because the three carboxylate groups have strong coordination affinity to Fe^{III} ions, which favors the attachment of citrate groups on the surface of the magnetite nanocrystals and prevents them from aggregating into large single crystals as occurred previously.^[30] Moreover, Na₃Cit is widely used in food and drug industry and citric acid is one of products from tricarboxylic acid cycle (TAC), a normal metabolic process in human body. Typically, the 250 nm magnetite particles were synthesized with the composition of FeCl₃/Na₃Cit/NaOAc/EG = 1:0.17:36.5:89.5 at 200 °C for 10 h (see the Supporting Information for experimental details).

Scanning electron microscopy (SEM) images show that when the FeCl₃ concentration is in the range of 0.05 to 0.25 mol L⁻¹, all of the magnetite particles obtained have a nearly spherical shape and uniform size (Figure 1). The diameter of the spheres dramatically increases from 80 to 410 nm with the increase of FeCl₃ concentration, indicating that higher FeCl₃ concentrations can lead to a larger particle size. Transmission electron microscopy (TEM) (Figure 2a) reveals that the magnetite particles prepared from 0.2 mol L⁻¹ of FeCl₃ have a nearly uniform size of about 250 nm and spherical shape, which is in good agreement to the SEM results (Figure 1c). A TEM image at higher magnification

[*] J. Liu, Z. K. Sun, Dr. Y. H. Deng, Y. Zou, C. Y. Li, Dr. X. H. Guo, L. Q. Xiong, Y. Gao, Prof. Dr. F. Y. Li, Prof. Dr. D. Y. Zhao
Department of Chemistry, Shanghai Key Laboratory of Molecular Catalysis and Innovative Materials and Advanced Materials Laboratory, Fudan University
Shanghai 200433 (China)
Fax: (+86) 21-6564-1740
E-mail: yhdeng@fudan.edu.cn
dyzhao@fudan.edu.cn
Homepage: <http://homepage.fudan.edu.cn/~dyzhao/>

[**] This work was supported by the NSF of China (20721063, 2021140537, 20871030, 20890120), the State Key Basic Research Program of the PRC (2006CB932302), Shanghai Leading Academic Discipline Project (B108), Shanghai Rising Star program (08A14010), and the Doctoral Program Foundation of the State Education Commission of China (200802461013).



Supporting information for this article is available on the WWW under <http://dx.doi.org/10.1002/anie.200901566>.

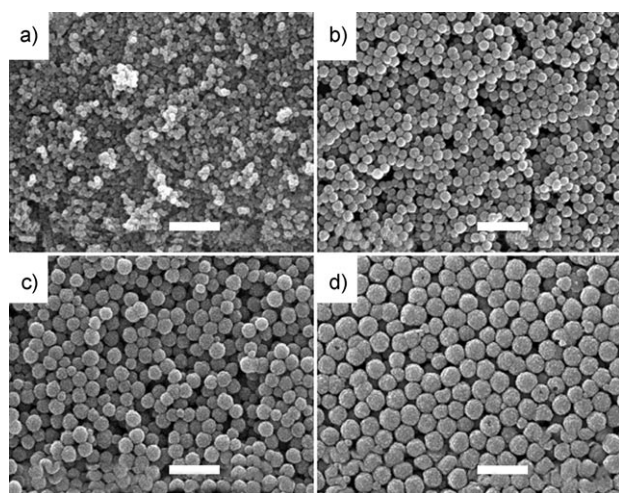


Figure 1. SEM images of Fe_3O_4 particles synthesized with different initial FeCl_3 concentrations: a) 0.05, b) 0.1, c) 0.2, and d) 0.25 mol L^{-1} . Scale bars: 1 μm .

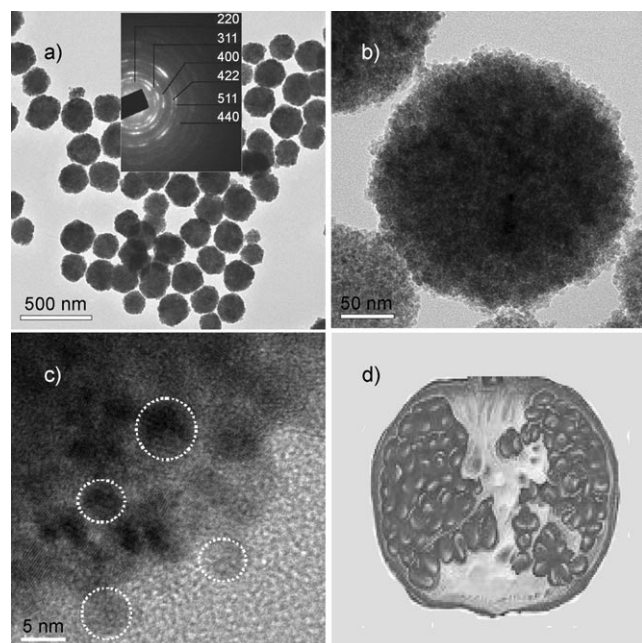


Figure 2. a) TEM images of 250 nm Fe_3O_4 particles and SAED pattern (inset), b) TEM image at higher magnification, c) HRTEM image, and d) a photograph of a pomegranate.

indicates that the obtained magnetite particles are loose clusters (Figure 2b), and a high-resolution TEM (HRTEM) image (Figure 2c) further reveals that the particles are composed of nanocrystals with the size of about 5–10 nm. Notably, as shown in the HRTEM image, these nanocrystals seem to be connected with each other by amorphous matrix as a bridge (Supporting Information, Figure S1). Selected-area electron diffraction (SAED) recorded on the edge of a magnetite particle shows polycrystalline-like diffraction, suggesting that it consists of many magnetite nanocrystals (Figure 2a, inset). This morphology may provide them with a

large surface area for adsorption of guest molecules, such as drug molecules. The structure of the magnetite particles is similar in appearance to a pomegranate (Figure 2d), in which seeds are packed into a large conglomeration.

Reaction parameters were investigated, including the reactant concentration and reaction temperature and time. The product obtained at a lower temperature (e.g., 190 °C) shows no magnetic response, indicating that 200 °C is a threshold temperature for forming magnetite using EG as a reductant.^[30] Without addition of Na_3Cit , the resultant product was single-crystal magnetite spheres (Supporting Information, Figure S2), which is similar to that reported by Li and co-workers.^[30] At 200 °C, the reaction time over a range of 5–12 h seems to have little effect on the mean diameters of the particles. However, as determined by SEM (Supporting Information, Figure S3), the particles become more uniform in size and shape as the reaction time increases. When the initial Na_3Cit concentration is increased from 20 to 51 mmol L^{-1} , the size of the obtained magnetite particles decreases from 300 to 170 nm (Supporting Information, Figure S4), indicating that higher Na_3Cit concentration can yield magnetite particles with smaller size. This trend agrees well with the increase in size with FeCl_3 concentration (Figure 1). Moreover, during washing the products with deionized water, the samples obtained with a high concentration of Na_3Cit show better water dispersibility. Our measurements reveal that with the increase of Na_3Cit concentration, the zeta potential ξ of the magnetite particles significantly decrease from -18.6 to -38.7 mV, implying the increase of negative charge density on the surface of particles as Na_3Cit concentration increases, and suggesting that Na_3Cit plays a vital role in the charge density on the surface. Considering the strong complexation with the Fe^{3+} ions, the citrate groups could anchor on the particle surface during the solvothermal reaction, and thus enhance the dispersibility of the magnetite particles.

FT-IR spectra of the magnetite particles obtained with Na_3Cit (Supporting Information, Figure S5) show absorption bands at 1652 and 1396 cm^{-1} associated with carboxylate, further indicating the existence of carboxyl groups. Thermogravimetric (TG) analysis in N_2 (Supporting Information, Figure S6) shows a large weight loss of about 12.2 wt % in the range of 100–800 °C for the 250 nm magnetite particles. In contrast, a weight loss of only 3.0 wt % is observed for the magnetite particles obtained without addition of Na_3Cit , implying that considerable amount of organic species is occluded in the former. Owing to the electrostatic repulsion effect, the magnetite particles can be easily dispersed in water, alcohol, and tetrahydrofuran to form a stable dispersion that can stand for 72 h without visible sedimentation (Supporting Information, Figure S5 inset). When a magnet (4000 Oe) is applied, the magnetite particles can be separated from their dispersion rapidly in only 1 min (Supporting Information, Videos S1 and S2). By adjusting the position of the magnet, the typical macroscopic chain-like structure related to the superparamagnetic behavior of the magnetic particles can be observed. Once the magnet is withdrawn, the particles can be redispersed into the water immediately by slight shaking. By contrary, the single-crystal magnetite

particles obtained without Na_3Cit show poor water dispersibility (Supporting Information, Video S3). The magnetic properties of all the magnetite particles synthesized with Na_3Cit over the concentration range $8.5\text{--}68\text{ mmolL}^{-1}$ indicate that the particles have no remanence or coercivity at 300 K, and their magnetization saturation value (M_s) increases with the decrease of Na_3Cit concentration. For example, the samples obtained with Na_3Cit concentration of 17, 34, and 68 mmolL^{-1} have magnetization saturation values (M_s) of 78.9, 73.6, and 56.2 emu g^{-1} , respectively (Figure 3A). This result suggests that lower citrate concentration favors the formation of magnetite particles with better crystallinity. Prolonging the reaction time from 6 to 12 h can increase the

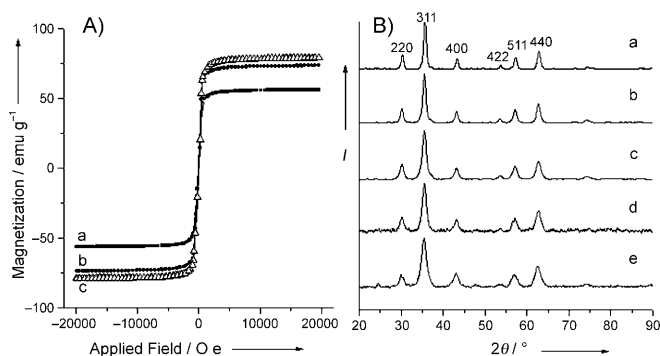


Figure 3. A) Hysteresis loops of Fe_3O_4 particles obtained with Na_3Cit concentrations of a) 68, b) 34, and c) 17 mmolL^{-1} . B) XRD patterns of Fe_3O_4 particles obtained with Na_3Cit concentrations of a) 8.5, b) 17, c) 34, d) 51, and e) 68 mmolL^{-1} .

magnetization from 62 to 78 emu g^{-1} (Supporting Information, Figure S7), but it slightly decreases the water dispersibility of the magnetite particles. This effect is probably caused by the abscission of citrate groups during the further crystallization of the magnetite particles. The blocking temperature of the 250 nm magnetite particles was measured to be 94 K (Supporting Information, Figure S8). The samples obtained with different Na_3Cit concentrations show typical X-ray diffraction (XRD) patterns of magnetite (JCPDS no. 19-629; Figure 3B). The broad diffraction peaks further suggests the nanocrystalline structure of the magnetite particles. As the Na_3Cit concentration increases, the broadening in the diffraction peaks becomes more pronounced. Based on the calculations with the Debye–Scherrer formula for the strongest 311 diffraction peak, the grain size of the magnetite particles decreases dramatically from 10.8 to 6.6 nm when the initial Na_3Cit concentration increases from 8.5 to 68 mmolL^{-1} , suggesting that Na_3Cit can significantly suppress the crystal growth of the grains. TEM observations provide an additional evidence for the suppression (Supporting Information, Figure S9). The diffraction peaks of the magnetite particles become narrow as the reaction time prolongs, which is indicative of an increase in crystallization (Supporting Information, Figure S10). An X-ray photoelectron spectrum (Supporting Information, Figure S11) shows peaks at 711.8 and 724.8 eV, which are in good agreement with the known values of the $\text{Fe}2p_{3/2}$ and $\text{Fe}2p_{1/2}$ oxidation states,

respectively.^[30] The results further confirm that the magnetite particles have been successfully synthesized by the facile modified solvothermal reaction.

The magnetite particles undergo a two-stage growth process. Once supersaturation for nucleation is achieved, the primary nanoparticles nucleate and gradually aggregate into large particles at high temperature.^[6] This process is different from thermal decomposition in that the highly single-crystalline nanocrystals generated by the “burst nucleation” are usually tightly coated by long-chain steric stabilizer (e.g., oleic acid). As a result, the nanocrystals cannot aggregate to form large particles. During the solvothermal process in this study, the Fe^{3+} ions undergo NaOAc -promoted hydrolysis and then are partially reduced to Fe_3O_4 primary nanoparticles by EG assisted with Na_3Cit . The primary Fe_3O_4 nanoparticles then gradually aggregate into large particles to minimize the surface energy. A similar result was observed by Ge et al.,^[32] who used PAA ($M_n = 1800\text{ g mol}^{-1}$) as a stabilizer and obtained 30–180 nm colloidal nanoclusters consisting of many primary magnetite nanoparticles. In our case, we found it easy to prepare magnetite particles over the size range 80–410 nm, but difficult to obtain particles smaller than 80 nm. The difference in the accessibility of the size of magnetite particles may stem from the difference in the stabilizing ability between PAA and citrate. The small-molecule citrate groups can anchor on the primary nanoparticles as the PAA does, and prevent the nanocrystals from growing further into large single crystals. However, in contrast to citrate groups, the PAA molecules undergo stronger complexation with Fe^{3+} ions, and the resultant particles have more intense electrostatic repulsion because there are many carboxylate groups in one polymer chain. This makes the primary nanoparticles aggregate into colloidal nanoclusters (30–180 nm), which are smaller than our magnetite particles (80–410 nm).

To examine the feasibility of the obtained magnetite particles in bio-related fields, the cytotoxicity was investigated (see the Supporting Information). The effect of the magnetite particles (250 nm) on cell proliferation was assessed with human nasopharyngeal epidermal carcinoma cells (KB cells) by means of a methyl thiazolyl tetrazolium (MTT) assay (Figure 4). The viability of untreated cells was assumed to be 100%. Notably, the cell viability still remains above 90% when they were incubated with magnetite particles of different concentrations for 6 h. Upon incubating the KB cells with the magnetite particles (0.2 mg mL^{-1}), less than 15% of the cells died after a 12 h exposure. Even when the concentration was increased to 2.0 mg mL^{-1} , the cell viability still remains above 80%. These results clearly indicate that our synthesized magnetite particles have low cytotoxicity.^[23]

By utilization of the citrate groups and high dispersibility, the as-synthesized magnetite particles can be easily functionalized further for various biomedical applications. The cell permeability of the obtained magnetite particles were investigated by using fluorescein isothiocyanate (FITC) as a tracer. A very small amount of FITC probe was used to modify the magnetite particles (250 nm) to produce bifunctional magnetic fluorescent colloids (see the Supporting Information). A fluorescent microscopy image (Figure 5a) shows that the FITC–magnetite particles are well-dispersed and have high

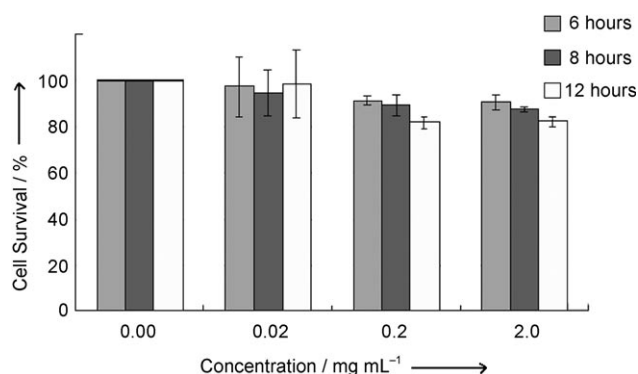


Figure 4. The in vitro cell viability of KB cells incubated with 250 nm Fe₃O₄ particles at different concentrations for 6–12 h.

luminescent intensity, suggesting that the particles were successfully modified with FITC molecules. The in vitro cell imaging test was carried out by using the human cervical carcinoma HeLa cell line (see the Supporting Information). After staining with FITC-magnetite particles for 2 h at 37 °C, the HeLa cells show intense intracellular luminescence (Figure 5b). The bright-field measurements indicate that the cells are viable during the staining process and imaging experiments, suggesting a good biocompatibility of the particles (Figure 5c). Overlays of the confocal luminescence and bright-field images show that the luminescence is from the intracellular region, revealing that the FITC-magnetite particles can penetrate into the living cells (Figure 5d).

Inspired by the above results, we further studied the application feasibility of the magnetite particles as separation tools for enrichment of trace peptides. Angiotensin II (Ang II) and Cytochrome *c* (Cyt *c*) digest were used to

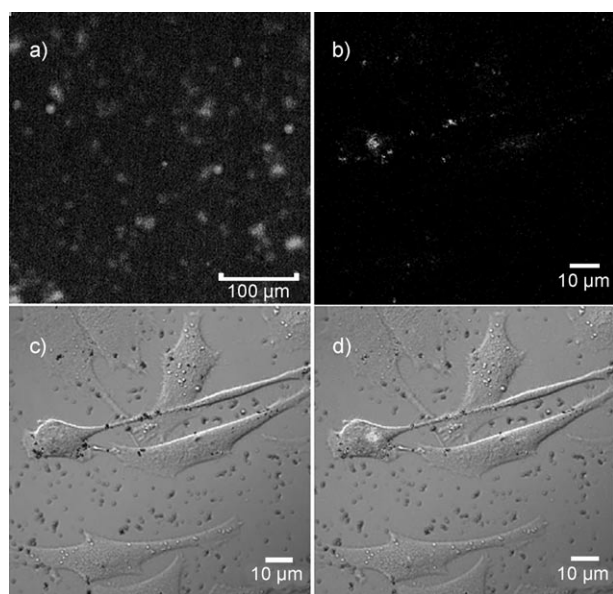


Figure 5. a) Fluorescent microscopy image of the FITC-magnetite particles deposited on a glass slide. b) Confocal luminescence images of HeLa cells stained with FITC-magnetite particles for 2 h at 37 °C. ($\lambda_{\text{ex}} = 488 \text{ nm}$), c) the corresponding bright-field image of the cells, and d) an overlay of the images in (b) and (c).

study the enrichment efficiency of the magnetite particles (250 nm) for peptides analysis using matrix-assisted laser desorption/ionization time-of-flight mass spectrometry (MALDI-TOF MS; Supporting Information, Figures S11, S12, Table S1). The Ang II was used to investigate the concentration factor; at the concentration of 5 fmol μL^{-1} , it was scarcely detected by MS with signal-to-noise (S/N) ratio of only 18.60. However, after enrichment with the magnetite particles, the peak intensity of Ang II becomes much higher, with a S/N ratio up to 921.55, indicating a concentration factor of about 50. The enrichment universality of the magnetite particles was evaluated by using 5 fmol μL^{-1} Cyt *c* digests. Without enrichment, no peak from Cyt *c* was observed because of a very low concentration. In contrast, after the enrichment by the magnetite particles, ten peaks were observed with high intensities. The results show that the magnetite particles with surface citrate groups can effectively enrich peptides at trace level.

In summary, a modified solvothermal approach was used to synthesize highly water-dispersible magnetite particles with uniform size by using citrate as a stabilizer. The particle size can easily be tuned over a wide range of 80–410 nm by varying the concentration of FeCl₃ or Na₃Cit. The reaction temperature is a key issue in preparing the uniform magnetite spheres by the citrate-modified solvothermal reductive reaction; the higher the temperature, the larger the particle size. The particles are composed of numerous primary magnetite nanocrystals with sizes of 5–10 nm, which render them superparamagnetism and high magnetization of 56–82 emu g⁻¹. The magnetite particles have a high magnetization, which enhances their response to external magnetic field and therefore should greatly facilitate the manipulation of the particles in practical uses. More importantly, owing to the presence of the citrate groups attached on the surface, the magnetite particles not only have excellent water dispersibility and dispersing stability, but also exhibit a low cytotoxicity, a good biocompatibility, and high capacity for efficient and convenient enrichment of trace peptides, which make them promising candidates for applications in various bio-related fields, such as cell imaging and cell sorting, and for sample pre-enrichment to analyze trace peptides or proteins in proteomics, and in particular those related with diseases, and to find biomarkers.

Received: March 23, 2009

Published online: July 3, 2009

Keywords: biocompatibility · colloids · magnetite · nanocrystals · superparamagnetism

- [1] Y. Yin, A. P. Alivisatos, *Nature* **2005**, 437, 664.
- [2] Z. A. Peng, X. G. Peng, *J. Am. Chem. Soc.* **2002**, 124, 3343.
- [3] Y. Sun, Y. N. Xia, *Science* **2002**, 298, 2176.
- [4] X. Wang, J. Zhuang, Q. Peng, Y. D. Li, *Nature* **2005**, 437, 121.
- [5] M. P. Pileni, *Nat. Mater.* **2003**, 2, 145.
- [6] J. Park, J. Joo, S. G. Kwon, Y. J. Jang, T. Hyeon, *Angew. Chem.* **2007**, 119, 4714; *Angew. Chem. Int. Ed.* **2007**, 46, 4630.
- [7] Y. W. Jun, J. W. Seo, J. Cheon, *Acc. Chem. Res.* **2008**, 41, 179.

- [8] C. Xu, K. Xu, H. Gu, R. Zheng, H. Liu, X. Zhang, Z. Gao, B. Xu, *J. Am. Chem. Soc.* **2004**, *126*, 9938.
- [9] Q. A. Pankhurst, J. Connolly, S. K. Jones, J. Dobson, *J. Phys. D* **2003**, *36*, R167.
- [10] M. Ferrari, *Nat. Rev. Cancer* **2005**, *5*, 161.
- [11] S. I. Stoeva, F. W. Huo, J. S. Lee, C. A. Mirkin, *J. Am. Chem. Soc.* **2005**, *127*, 15362.
- [12] M. G. Harisinghani, J. Barentsz, P. F. Hahn, W. M. Deserno, S. Tabatabaei, C. H. Van de Kaa, J. De La Rosette, R. Weissleder, *N. Engl. J. Med.* **2003**, *348*, 2491.
- [13] Y. M. Huh, Y. Jun, H. T. Song, S. J. Kim, J. S. Choi, J. H. Lee, S. Yoon, K. S. Kim, J. S. Shin, J. S. Suh, J. Cheon, *J. Am. Chem. Soc.* **2005**, *127*, 12387.
- [14] S. J. Son, J. Reichel, B. He, M. Schuchman, S. B. Lee, *J. Am. Chem. Soc.* **2005**, *127*, 7316.
- [15] R. Weissleder, A. Moore, U. Mahmood, R. Bhorade, H. Benveniste, E. A. Chiocca, J. P. Bacion, *Nat. Med.* **2000**, *6*, 351.
- [16] M. Lewin, N. Carlesso, C. H. Tung, X. W. Tang, D. Cory, D. T. Scadden, R. Weissleder, *Nat. Biotechnol.* **2000**, *18*, 410.
- [17] J. Kim, S. Park, J. E. Lee, S. M. Jin, J. H. Lee, I. S. Lee, I. Yang, J. S. Kim, S. K. Kim, M. H. Cho, T. Hyeon, *Angew. Chem.* **2006**, *118*, 7918; *Angew. Chem. Int. Ed.* **2006**, *45*, 7754.
- [18] N. Rosi, C. A. Mirkin, *Chem. Rev.* **2005**, *105*, 1547.
- [19] a) Y. K. Hahn, Z. Jin, H. Kang, E. Oh, M.-K. Han, H.-S. Kim, J.-T. Jang, J. H. Lee, J. Cheon, S. H. Kim, H. S. Park, J. K. Park, *Anal. Chem.* **2007**, *79*, 2214; b) Y. H. Deng, D. W. Qi, C. H. Deng, X. M. Zhang, D. Y. Zhao, *J. Am. Chem. Soc.* **2008**, *130*, 28.
- [20] J. Kim, J. E. Lee, J. Lee, J. H. Yu, B. C. Kim, K. An, Y. Hwang, C. H. Shin, J. G. Park, J. Kim, T. Hyeon, *J. Am. Chem. Soc.* **2006**, *128*, 688.
- [21] A. Jordan, R. Scholz, P. Wust, H. Fahling, R. Felix, *J. Magn. Mater.* **1999**, *201*, 413.
- [22] Y. W. Jun, Y. M. Huh, J. S. Choi, J. H. Lee, H. T. Song, S. Kim, S. Yoon, K. S. Kim, J. S. Shin, J. S. Suh, J. Cheon, *J. Am. Chem. Soc.* **2005**, *127*, 5732.
- [23] M. Babincova, P. Sourvong, D. Leszczynska, P. Babinec, *Med. Hypotheses* **2000**, *55*, 459.
- [24] A. H. Lu, E. L. Salabas, F. Schüth, *Angew. Chem.* **2007**, *119*, 1242; *Angew. Chem. Int. Ed.* **2007**, *46*, 1222.
- [25] a) T. Hyeon, S. S. Lee, J. Park, Y. Chang, H. B. Na, *J. Am. Chem. Soc.* **2001**, *123*, 12798; b) N. R. Jana, Y. Chen, X. G. Peng, *Chem. Mater.* **2004**, *16*, 3931; c) S. H. Sun, H. Zeng, *J. Am. Chem. Soc.* **2002**, *124*, 8204; d) J. Park, K. An, Y. Hwang, J. G. Park, H. J. Noh, J. Y. Kim, J. H. Park, N. M. Hwang, T. Hyeon, *Nat. Mater.* **2004**, *3*, 891.
- [26] C. Xu, K. Xu, H. Gu, X. Zhong, Z. Guo, R. Zheng, X. Zhang, B. Xu, *J. Am. Chem. Soc.* **2004**, *126*, 3392.
- [27] a) C. Xu, K. Xu, H. Gu, R. Zheng, H. Liu, X. Zhang, Z. Guo, B. Xu, *J. Am. Chem. Soc.* **2004**, *126*, 9938; b) M. D. Shultz, J. U. Reveles, S. N. Khanna, E. E. Carpenter, *J. Am. Chem. Soc.* **2007**, *129*, 2482.
- [28] R. Hong, N. O. Fischer, T. Emrick, V. M. Rotello, *Chem. Mater.* **2005**, *17*, 4617.
- [29] R. De Palma, S. Peeters, M. J. van Bael, H. V. van den Rul, K. Bonroy, W. Laureyn, J. Mullens, G. Borghs, G. Maes, *Chem. Mater.* **2007**, *19*, 1821.
- [30] H. Deng, X. Li, Q. Peng, X. Wang, J. Chen, Y. D. Li, *Angew. Chem.* **2005**, *117*, 2842; *Angew. Chem. Int. Ed.* **2005**, *44*, 2782.
- [31] F. Bai, D. S. Wang, Z. Y. Huo, W. Chen, L. P. Liu, X. Liang, C. Chen, X. Wang, Q. Peng, Y. D. Li, *Angew. Chem.* **2007**, *119*, 6770; *Angew. Chem. Int. Ed.* **2007**, *46*, 6650.
- [32] J. P. Ge, Y. X. Hu, M. Biasini, W. P. Beyermann, Y. D. Yin, *Angew. Chem.* **2007**, *119*, 4420; *Angew. Chem. Int. Ed.* **2007**, *46*, 4342.